

Monoclinic ray trace synthetics

Scott Leaney and Chris Chapman, Schlumberger

Summary

Geological layering at all scales causes polar or VTI elastic anisotropy while vertical fractures and/or horizontal stress anisotropy add an azimuthal variation in properties. The addition of fractures and/or horizontal stress anisotropy to a background VTI medium results in a medium with orthorhombic symmetry. Regional stress direction may change with depth or fracture sets may be non-aligned with the regional stress direction, it is therefore of interest to simulate offset- and azimuth- dependent reflection amplitudes in a 1D layered model with orthorhombic properties and a symmetry axis direction that varies with depth. Such a model requires a monoclinic treatment. We utilize exact anisotropic ray theory to compute ray paths, times and reflection amplitudes. After a theoretical description we show results of two-point ray tracing through the SEAM 2 Barrett 1D model, which contains a depth-variable symmetry axis direction. This model is very well approximated by a vertically fractured, VTI layered medium and serves to illustrate some interesting features. We observe significant out-of-plane refraction and very large reflection time variations with azimuth. These are due to a very large normal-to-shear fracture compliance ratio (Z_n/Z_t) in the model. We also observe relatively weak azimuthal AVA, which we attribute to the relatively weak (*and negative*) contrast in azimuthal anisotropy in the shale reservoirs. We compute offset-azimuth gathers and compare nearest VTI to exact monoclinic NMO corrections. Monoclinic dynamic ray trace synthetics provide an efficient tool for AVAz well tie and inversion algorithm development.

Introduction

Amplitude variation with azimuth (AVAz) has evolved from an interesting attribute to a goal of quantitative inversion (Lynn et al., 1995; Downton, 2011; Bachrach, 2014). Workflows have been developed to build predictive geomechanical models from the results of orthorhombic AVAz inversion (Sayers and den Boer, 2018), but the inversions assumed a constant symmetry axis orientation. A depth-variable symmetry axis orientation or multiple vertical fracture sets require a monoclinic treatment, and while monoclinic AVAz has been studied (Sayers and Dean, 2001), as far as we know the latest orthorhombic inversions have been limited to a symmetry axis direction that is constant with time or depth (Gofer et al., 2016). The challenge posed by the SEAM Phase 2 model (Van De Coevering et al., 2019) also requires a monoclinic treatment. Given the efficiency and utility of ray theory, it is of interest to consider a 1D layered medium with monoclinic symmetry as such a treatment will allow the simulation of a model with depth-dependent symmetry axis. Here we make use of the efficiencies afforded by simplifying from general triclinic anisotropy to 1D layered media with a single (horizontal) plane of mirror symmetry – monoclinic media. We use the SEAM phase 2 Barrett 1D model to illustrate some interesting ray trace attributes and show synthetic data.

Theoretical discussion

The algorithm behind the 1D monoclinic ray tracer is summarized here. For mathematical details of general anisotropic ray tracing see Chapman (2004). In anisotropic media the directions of phase, group and polarization are not simply aligned. In a 1D layered medium the horizontal components of phase slowness $\mathbf{p}=(p_1, p_2)$ are constant everywhere along a ray path. Ray tracing in general requires solving an eigen problem given \mathbf{p} and the density-normalized stiffness tensor,

A_{ij} , of the layer. The eigenvalues correspond to the vertical components of phase slowness (p_3) and the polarizations are obtained from the eigenvectors. Given the completed phase slowness and polarization vectors the group velocity vector can be computed. The group velocity defines the ray direction which allows the ray to be traced through a layer of thickness z_i , and the lateral position (x,y) is accumulated in the sum over layers.

Two-point ray tracing involves iteratively altering the take-off direction from the source to find the ray that lands tolerably close to a receiver. Regarding the nonlinear problem of 2-point ray tracing, when layers are isotropic or VTI then \mathbf{p} is a single parameter and iterative two-point ray tracing is very efficient at finding the target offset or range through a stack of layers, but when the symmetry of a layer includes an azimuthal variation in velocity then \mathbf{p} is a 2-vector and the two-point optimization problem is much more expensive. It is therefore of interest to reduce the computational burden required in any layer. Considering a medium with up-down symmetry – a monoclinic medium – reduces the matrix eigen problem from 6x6 to 3x3, taking roughly 1/8th the compute time. This is the symmetry that we consider here.

The 1D model may be represented using a variety of parameterizations, for example Tsvankin's parameters (Tsvankin, 1997) or the crack compliance parameters of Schoenberg and Helbig (1997) together with the fast azimuth direction. The 13 monoclinic stiffness moduli may also be used. Whatever the model parameterization, it is pre-processed to extract a computational 1D model given source, receiver and optionally reflector depths. In any layer there may be two shear rays so a ray signature that includes a layer with a shear segment requires some discussion. Although labelling the eigenvalues and eigenvectors according to phase speed is a straightforward approach to shear labelling, it may not be terribly useful. We do shear labelling based on polarization, for example the polarization that is closest to the corresponding shear of the nearest isotropic medium. The shear group velocity corresponding to the selected shear ray signature in the layer (qSv or qSh) is thus used for the ray. There is no perfect shear labelling strategy and due to the singularities in low symmetry slowness surfaces two-point ray trace failures can occur for rays containing a shear segment.

The two-point monoclinic ray tracing problem is a nonlinear search for the two parameters $\mathbf{p}=(p_1,p_2)$ that will land the ray on the receiver $\mathbf{r}=(r_1,r_2,r_3)$. We use a hybrid optimization strategy similar to that described in Leaney (2014) that includes numerical gradients and bisection. Once \mathbf{p} has been determined the times and amplitudes can be computed. The reflection and transmission coefficients are accumulated along the ray, as is geometrical spreading. Polarizations are saved at source and receiver for use in source radiation and receiver response which may include interface conversions, to handle, for example, a free surface. Since the medium is composed of homogeneous layers there are no caustics due to velocity gradients but complex transmission and reflection coefficients are accumulated and included at wavelet convolution. Presently Q is not treated anisotropically but each of the three ray codes in a layer (qP, qSv, qSh) may have different Q values and the time-harmonic average Q value is returned for use in wavelet convolution.

Having described the monoclinic ray tracer we now show some results using the SEAM Phase II Barrett 1D model.

SEAM Phase II Barrett model

The SEAM Phase II (SP2) model contains structural and stratigraphic features and a complex statics layer with absorptive properties for shear (Regone et al., 2017), we use a central well

location where 1D properties have been documented (Oristaglio, 2015); more details can be found in the SEAM Phase II public documentation (2018). The SP2 model is orthorhombic in every layer and was built by combining a VTI background gradient with HTI properties defined in terms of Thomsen TI parameters. The HTI component has a different orientation in the reservoirs compared to the rest of the layers. The method used for combining the VTI and HTI properties uses the idea of compliance tensor summation (e.g. Schoenberg and Sayers, 1995) and does not rely on linear slip theory (Oristaglio, 2015). Following the procedure described by Hood and Schoenberg (1989) to decompose an orthorhombic tensor as a fractured VTI (FVTI) medium, we found that the normalized distance from a FVTI model is very small, being everywhere less than 0.012 and generally less than 0.005, so we use FVTI parameters to represent model properties. The normal-to-shear fracture compliance ratio (Z_n/Z_t) from FVTI tensor decomposition exceeds 0.75 at all depths, considered physically implausible (Sayers, pers.comm.), but this provides a strong azimuthal variation in P-p reflection times. A workflow to build realistic FVTI models based on the upscaling of sonic anisotropy logs was discussed last year (Leaney et al., 2019).

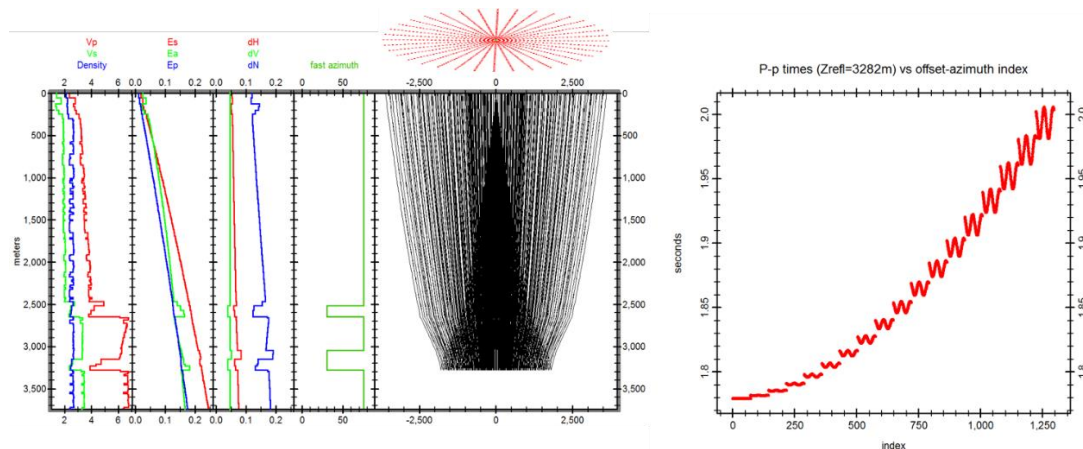


Figure 1. Left: The SEAM 2 model shown as FVTI parameters with qP-p rays for a circular grid of shot points out to an offset/depth ratio of 1. Right: P-p times versus increasing offset and azimuth.

Results

A multi-offset, multi-azimuth survey was constructed to compute attributes with the monoclinic ray tracer. A source (receiver) was placed at (0,0,0) and then offset rings of receivers were placed at increasing radii. Figure 1 shows rays in section from the south with the model expressed as FVTI parameters. Also shown are reflection times for increasing offset and azimuth. For this case the maximum offset corresponded to an offset-to-depth ratio of about 1 for the deepest base reservoir reflector at 3282m. Figure 2 shows ray trace reflection coefficients for the base reservoir reflector for a maximum offset of 4200m. Displays are at reflection point; versus incident phase polar and azimuth angle; and versus polar incidence angle for all azimuths. Note the change in maximum incident angle as a function of azimuth. Figure 3 shows different symmetric and asymmetric ray paths for an offset of 4200m at a source-receiver azimuth of N115E. This shows that significant out-of-plane refraction occurs (20m for P-p, this also impacts the azimuth incident angle). Figure 4 shows time-based model properties and offset-azimuth gathers where eight azimuths were computed for a range of offsets out to 4km. Shown are the results of NMO correction using the nearest VTI model and exact orthorhombic model with depth-variable fast azimuth.

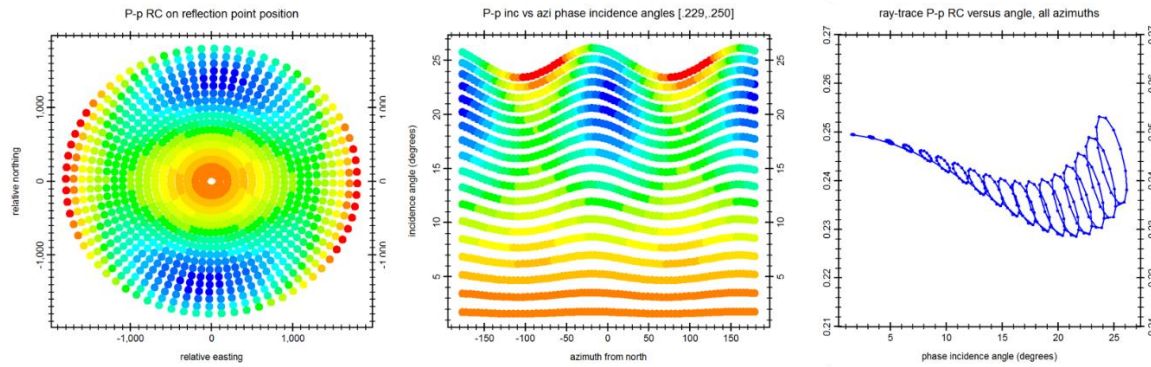


Figure 2. Ray trace AVAz for the base Eagleford reflector. Left: Reflection coefficients (RC) on (x,y) reflection point position; middle: RC versus phase incidence polar and azimuth angle; right: RC versus incidence angle for all azimuths.

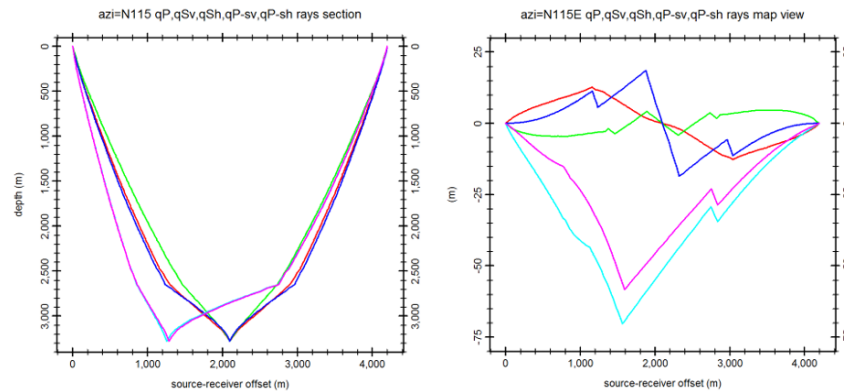


Figure 3. qP-p(blue), qSv-sv(green), qSh-sh(red), qP-sv(magenta), qP-sh(cyan) ray paths in section (left) and in map view (right) for an azimuth N115E and offset=4200.

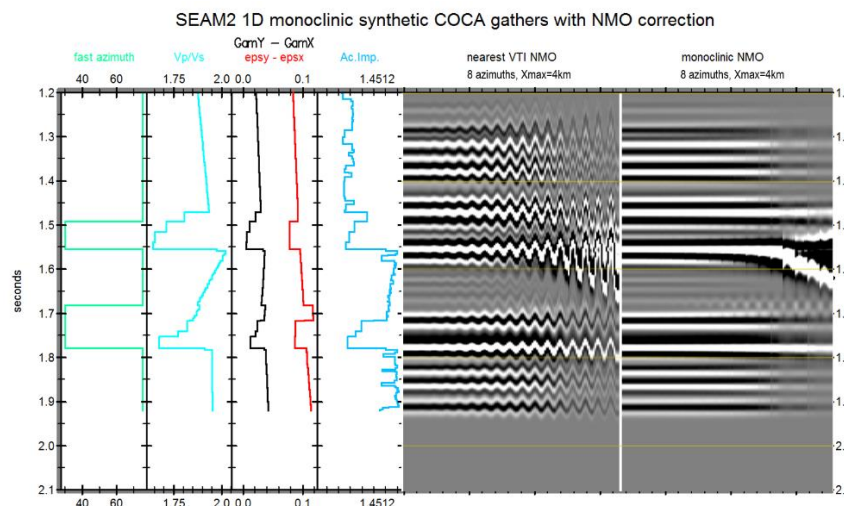


Figure 4. Time-based model attributes including from left to right: orthorhombic fast azimuth, Vp/Vs, linearized ortho AVA parameters and Ac.Imp. Synthetic offset-azimuth gathers are shown with nearest VTI model NMO correction (left) and exact monoclinic NMO correction (right).

Conclusions

A dynamic anisotropic ray tracing algorithm was described for 1D models with homogeneous layers and symmetry as low as monoclinic. The treatment is exact, providing out-of-plane refraction in ray paths. We illustrated the algorithm by using the SEAM Phase 2 Barrett 1D model, which contains orthorhombic layers with depth-variable fast azimuth direction and was found to be very well approximated by vertically fractured VTI properties. Time and amplitude attributes were computed for the deep base reservoir reflector. Synthetic offset-azimuth gathers were computed and NMO correction applied using nearest VTI and monoclinic models to illustrate the utility of the functionality. 1D monoclinic ray tracing has many uses in conjunction with AVAZ inversion and full wave synthetic packages.

Acknowledgements

Thanks to Edan Gofer, Colin Sayers, Bruce Hootman, Rafael Guerra and to the SEG SEAM Phase II consortium.

References

- Bachrach, R., 2014, Linearized orthorhombic AVAZ inversion: Theoretical and practical consideration: SEG Expanded Abstracts.
- Chapman, C.H., 2004, Fundamentals of Seismic Wave Propagation, Cambridge University Press.
- Downton, J., 2011, Azimuthal Fourier coefficients: A simple method to estimate fracture parameters: SEG, Expanded Abstracts.
- Gofer, E., Bachrach, R., Fletcher, R. and Vie, M., 2016, Nonlinear orthorhombic AVAZ inversion workflow: SEG Expanded Abstracts.
- Hood, J.A. and Schoenberg, M., 1989, Estimation of vertical fracturing from measured elastic moduli: *Journal of Geophysical Research*, **94**, B11, 15611-15618.
- Leaney, W.S., 2014, Microseismic source inversion in anisotropic media: PhD Thesis, University of British Columbia.
- Leaney, S., Velez, E., Lawton, D and Innanen, K., 2019, Sonic anisotropy and monoclinic model building at the CaMI site: Geoconvention.
- Lynn H.B., Bates C.R., Layman M. and Jones M. 1995. Natural fracture characterization using P-wave reflection seismic data, VSP, borehole imaging logs and in-situ stress field determination. *SPE* 29595.
- Oristaglio, M., 2015, SEAM update: Elastic anisotropy in SEAM Phase II models: The Leading Edge, **34**, no. 8, 964-970.
- Regone, C., J., Stefani, P., Wang, C., Gereaa, G., Gonzalez, and M., Oristaglio, 2017, Geologic model building in SEAM Phase II—Land seismic challenges: The Leading Edge, **36**, 738–749.
- Sayers, C.M. and Dean, S., 2001, Azimuth-dependent AVO in reservoirs containing non-orthogonal fracture sets: Geophysical Prospecting, **49**, 100-106.
- Sayers, C.M. and den Boer, L., 2018, Constructing a discrete fracture network using seismic inversion to predict elastic and seismic properties plus fluid-flow anisotropy: Geoconvention.
- Schoenberg, M. and Sayers, C.M., 1995, Seismic anisotropy of fractured rock: *Geophysics*, **60**, 204-211.
- Schoenberg, M., and K. Helbig, 1997, Orthorhombic media: Modeling elastic wave behavior in a vertically fractured earth: *Geophysics*, **62**, 1954-1974.
- SEAM Corporation, Phase II Barrett Model Public Documentation, 2018, <https://drive.google.com/file/d/1ngFn8xkAPT-2tcQgvARk6ntbnCchh86n/view>, accessed 31 January, 2020.
- Tsvankin, I., 1997, Anisotropic parameters and P-wave velocity for orthorhombic media: *Geophysics*, **62**, 1292-1309.